

Fig. 4. Cornea and retina development following lens transplantation. Sections through the (A to D) anterior sector and (E to H) retina of a surface fish (A and E), a cave fish (B and F), a cave fish host with a transplanted surface fish lens (C and G), and a surface host with a transplanted cave fish lens (D and H). CE, corneal epithelium; R, rhodopsin-positive rod cells. Other abbreviations are as in Figs. 1 through 3. Arrows in (F) indicate a small number of cells expressing rhodopsin in the cave fish retina. Scale bar in (A) is 150 μ m, and the scale bar in (E) is 100 μ m; magnification is the same in (A) to (D) and in (E) to (H).

ringer (CFZFR) [116 mM NaCl, 2.9 mM KCl, and 10 mM Hepes (pH 7.2)] containing 0.2% EDTA, rinsed in CFZFR (40°C), and embedded in 1.2% agar in CFZFR (40°C). After cooling to room temperature, individual embryos were cut into agarose blocks. The operations were done with sharp tungsten needles in agarose

blocks arranged side by side in CFZFR. The host embryos were grown to adults under the normal photoperiod.

11. Y. Gavrieli, Y. Sherman, S. A. Ben-Sasson, *J. Cell Biol.* **119**, 493 (1996).
12. In 81 transplantations, 38 (49%) of the hosts sur-

vived. Nineteen (50%) of the survivors showed large external eyes on the transplant side, and the remainder showed eyes buried in the skin, although they were larger than those on the control side.

13. R. Macdonald and S. W. Wilson, *Dev. Genes Evol.* **206**, 363 (1997).
14. Specimens were fixed in 4% paraformaldehyde, embedded in Paraplast, and sectioned at 8 μ m. Sections were microwaved in 10 mM citric acid at pH 6.0 (three times) for 5 min to expose the antigens before immunostaining (9). Pax6 antibody was purchased from Babco (Richmond, CA), PCNA antibody was purchased from Santa Cruz Biotechnology (Santa Cruz, CA), and rhodopsin antibody was purchased from Leinco Technologies (St. Louis, MO). S. I. Tomarev provided Prox 1 antibody. For primary incubations, the Pax6, Prox 1, and PCNA antibodies were diluted 100:1, and the rhodopsin antibody was diluted 50:1.
15. N. Hirsch and W. A. Harris, *J. Neurobiol.* **32**, 45 (1997).
16. Web fig. 1 is available at www.sciencemag.org/feature/data/1051074.shl.
17. M. Perron, S. Kanekar, M. L. Vetter, W. A. Harris, *Dev. Biol.* **199**, 185 (1998).
18. K. Negishi, W. K. Stell, Y. Takasaki, *Dev. Brain Res.* **55**, 121 (1990).
19. Of 31 transplantations, 15 (44%) of the hosts survived. Thirteen (87%) of the survivors showed small degenerate eyes on the transplant side, and the remainder showed no effects on eye development.
20. Our results are relevant only to the Pachón cave fish studied here, one of at least 30 *Astyanax* cave fish populations that may have evolved the eyeless phenotype by different mechanisms (4, 6).
21. This work was supported by NSF grant DEB 9726561 (to W.R.J.). We thank D. Heyser for technical assistance and K. Kan for discussion of histochemical methods.

6 April 2000; accepted 25 May 2000

Synaptic Integration Mediated by Striatal Cholinergic Interneurons in Basal Ganglia Function

Satoshi Kaneko,¹ Takatoshi Hikida,¹ Dai Watanabe,¹ Hiroshi Ichinose,² Toshiharu Nagatsu,² Robert J. Kreitman,³ Ira Pastan,³ Shigetada Nakanishi^{1*}

The physiological role of striatal cholinergic interneurons was investigated with immunotoxin-mediated cell targeting (IMCT). Unilateral cholinergic cell ablation caused an acute abnormal turning behavior. These mice showed gradual recovery but displayed abnormal turning by both excess stimulation and inhibition of dopamine actions. In the acute phase, basal ganglia function was shifted to a hyperactive state by stimulation and suppression of striatonigral and striatopallidal neurons, respectively. D1 and D2 dopamine receptors were then down-regulated, relieving dopamine-predominant synaptic perturbation but leaving a defect in controlling dopamine responses. The acetylcholine-dopamine interaction is concertedly and adaptively regulated for basal ganglia synaptic integration.

The basal ganglia subserve motor and cognitive functions (1–5), and damage to this structure leads to abnormalities such as Parkinson's disease and Huntington's disease (6–9). In the basal ganglia circuit, cortical information reaches separate subpopulations

of striatal γ -aminobutyric acid (GABA)-containing, medium-sized spiny neurons, which is then transmitted to substantia nigra pars reticulata (SNr)/entopeduncular nucleus (EPN) through two parallel routes named direct and indirect pathways (6, 10, 11). Striatonigral

neurons in the direct pathway and striatopallidal neurons in the indirect pathway contain substance P (SP) and enkephalin (Enk), respectively. The two striatal principal neurons are thought to exert opposing effects upon the SNr/EPN neurons and the dynamic balance of basal ganglia-thalamocortical circuitry.

Activity of striatal principal neurons is modulated by dopaminergic and cholinergic inputs (12–14). Dopamine (DA) from substantia nigra pars compacta neurons excites and inhibits striatonigral and striatopallidal neurons, respectively. Acetylcholine (ACh) from striatal cholinergic neurons, opposing the DA action, inhibits and excites striatonigral and striatopallidal neurons, respectively (13, 15, 16). The modulatory role of DA transmission in the basal ganglia circuit has been well characterized (12, 17–20), whereas the precise physiological and behavioral function of cholinergic neurons accounting for only 1 to 2% of the striatal neuronal

¹Department of Biological Sciences, Kyoto University Faculty of Medicine, Kyoto 606-8501, Japan. ²Institute for Comprehensive Medical Science, School of Medicine, Fujita Health University, Toyoake 470-1192, Japan. ³Laboratory of Molecular Biology, Division of Basic Science, National Cancer Institute, National Institutes of Health, Bethesda, MD 20892, USA.

*To whom correspondence should be addressed. E-mail: snakanis@phy.med.kyoto-u.ac.jp

populations (21) still largely remains to be determined. Here, we report the function of striatal cholinergic interneurons with IMCT technology that selectively ablated these neurons from the adult striatum.

We previously generated transgenic mice

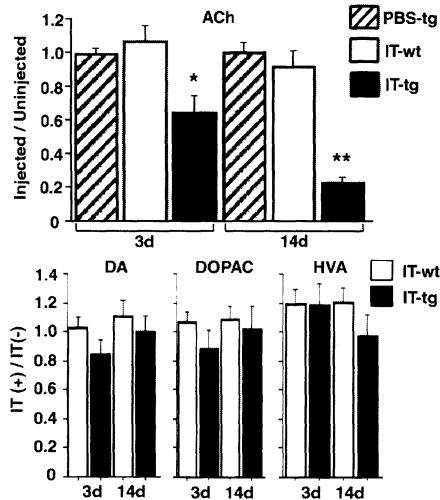


Fig. 1. Reduction of ACh levels with no alteration of DA and its metabolite levels in the cholinergic cell-ablated striatum. At days 3 and 14 after injection of IT or PBS into the left striatum, levels of ACh (**top**) and those of DA, DOPAC, and HVA (**bottom**) at the injected and uninjected sides of the striatum were measured. ACh levels were significantly reduced at the IT-injected side of the striatum on days 3 and 14 of IT-injected transgenic mice (IT-tg). For comparison, relative levels of the four compounds between the injected and uninjected sides of the striatum are presented (*, $P < 0.05$; **, $P < 0.01$; $n = 4$ to 9). Columns and error bars represent mean \pm SEM, respectively. PBS-tg, PBS-injected transgenic mice; IT-wt, IT-injected wild-type mice.

in which human interleukin-2 receptor α subunit (hIL-2R α) fused to green fluorescent protein (GFP) was expressed under the control of the mGluR2 promoter (22). Consistent with specific mGluR2 expression in large striatal neurons (23), double immunostaining showed the complete overlap of GFP-immunoreactive cells with choline acetyltransferase (ChAT)-immunoreactive cells (24). No GFP immunoreactivity was detected in any other striatal cell types (24).

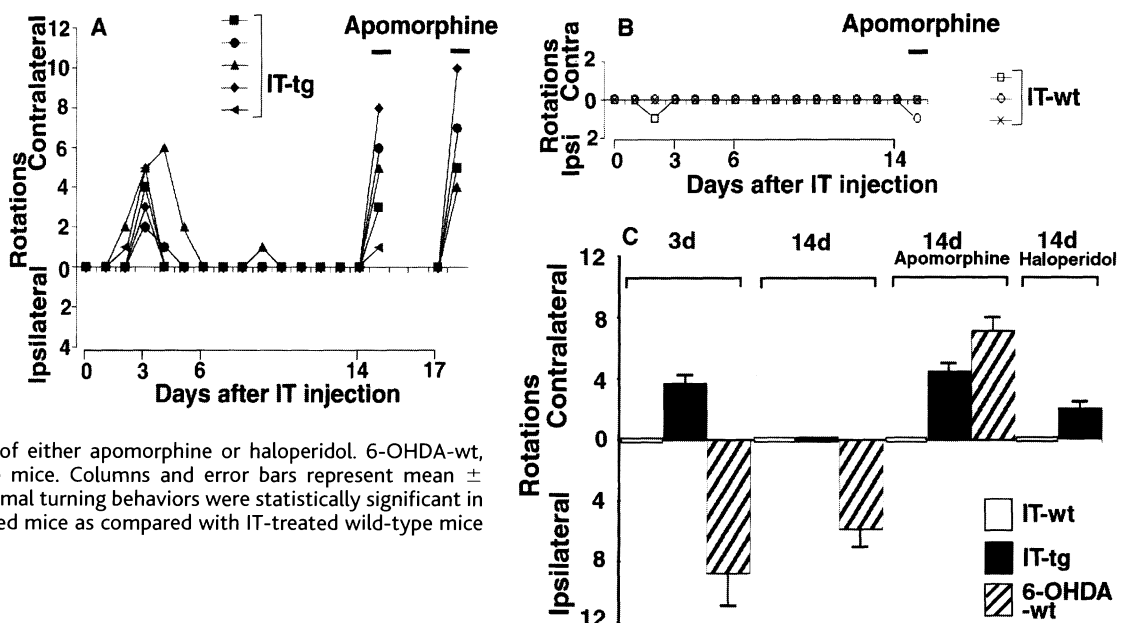
The immunotoxin (IT) is composed of monoclonal hIL-2R α antibody fused to bacterial toxin (25). After a survey of IT injection conditions, we chose to use five sites of injection on one side of the striatum (26). Serially dissected brain sections of adult transgenic mice 3 days after IT injection showed that GFP-immunoreactive cell bodies were visible but severely degenerated with a marked reduction in both GFP immunoreactivity and GFP-immunopositive dendritic fibers (27). Two weeks after IT injection, more than 80% of the cholinergic neurons were eliminated in transgenic mice (24). GFP-expressing cells outside the striatum were not ablated by IT treatment. Furthermore, ChAT-positive neurons were unaltered in wild-type mice treated with IT or in transgenic mice injected with phosphate-buffered saline (PBS) alone (27). Serial brain sections of IT-treated transgenic mice showed no anatomical change in any brain regions. Additionally, a distinct striatal cell population with parvalbumin immunoreactivity showed no reduction by IT injection (27). The pattern and intensity of dopamine transporter immunoreactivity on dopaminergic nerve terminals were also unchanged (27).

Intrastriatal levels of ACh levels were reduced to 64% on day 3 and further decreased

to 23% on day 14 after IT treatment of transgenic mice (Fig. 1) (28). The reduction of synaptic ACh levels at the acute phase could be underestimated because cholinergic cells were atrophied but were still visible at this stage. No ACh reduction was observed in either PBS-treated transgenic mice or IT-treated wild-type mice. Levels of DA and the DA metabolites, 3, 4-dihydroxyphenylacetic acid (DOPAC) and homovanillic acid (HVA), remained unchanged on both day 3 and day 14 of IT-treated transgenic and wild-type mice.

Unilaterally IT-treated transgenic mice survived for at least 6 months with no obvious change in locomotor activity. However, they frequently (~50%) showed an asymmetric concaving posture with a postural bending toward the IT-uninjected side 2 to 4 days after IT treatment. This behavioral abnormality was quantitatively investigated by forcing the animals to rotate on a hemispherical container and then measuring the rotating frequency (29). Unilaterally IT-injected transgenic animals, regardless of the presence and absence of a twisted posture, all showed rotations contralateral to the side of IT injection (Fig. 2A). This contralateral rotation became maximal 3 days after injection and began to disappear thereafter. The observed recovery of abnormal turning may result from an adaptive attenuation of DA transmission, which could relieve synaptic perturbation resulting from ACh depletion. We thus tested for the rotating behavior after enhancing DA transmission by subcutaneous injection of the DA agonist, apomorphine. The mice again showed contralateral rotation (Fig. 2A). IT-treated wild-type mice and PBS-injected transgenic mice never showed meaningful contralateral or ipsilateral rotation in the acute phase or

Fig. 2. Abnormal rotating after IT or 6-OHDA treatment. Numbers of rotations were measured daily after IT injection into the left striatum of individual transgenic (A) and wild-type (B) mice. At days 14 and 17, rotations were measured before and 15 min after apomorphine injection. (C) Rotating behaviors at day 3 ($n = 9$ to 19) and day 14 ($n = 6$ to 8) after IT or 6-OHDA injection into the left striatum. At day 14, rotations were measured before and 15 min after injection of either apomorphine or haloperidol. 6-OHDA-wt, 6-OHDA-injected wild-type mice. Columns and error bars represent mean \pm SEM, respectively. The abnormal turning behaviors were statistically significant in both IT- and 6-OHDA-treated mice as compared with IT-treated wild-type mice ($P < 0.05$).



REPORTS

after apomorphine administration in the chronic phase (Fig. 2B) (27).

Unilateral lesions of nigrostriatal DA neurons with 6-hydroxydopamine (6-OHDA) microinjection induce ipsilateral rotation reflecting a hypoactive state of the DA-depleted side of the striatum (30). Apomorphine administration conversely evokes contralateral rotation by activating supersensitized DA receptors after persistent DA depletion (30). Rotation was compared between 6-OHDA-lesioned and IT-treated animals (Fig. 2C).

DA-depleted animals showed severe, long-lasting ipsilateral rotation, and this rotation was reversed by apomorphine administration. IT-treated animals, on the contrary, showed contralateral rotation in the acute phase, followed by recovery in the chronic phase. This recovery suggests a compensation of imbalanced motor movement rather than changes in motor learning. However, addition of apomorphine produced contralateral rotation in the chronic phase. We also tested for the ability of chronically IT-treated transgenic

mice to respond to reduced DA transmission after application of the DA antagonist, haloperidol. Although haloperidol reduced locomotor activity in both wild-type and cholinergic cell-eliminated mice, an abnormal contralateral turning was induced only in the unilaterally cholinergic cell-eliminated mice (Fig. 2C).

The levels of SP and Enk mRNAs are known to be up- or down-regulated in the striatal principal neurons, depending on whether the striatonigral and striatopallidal neurons become hyperactive or hypoactive,

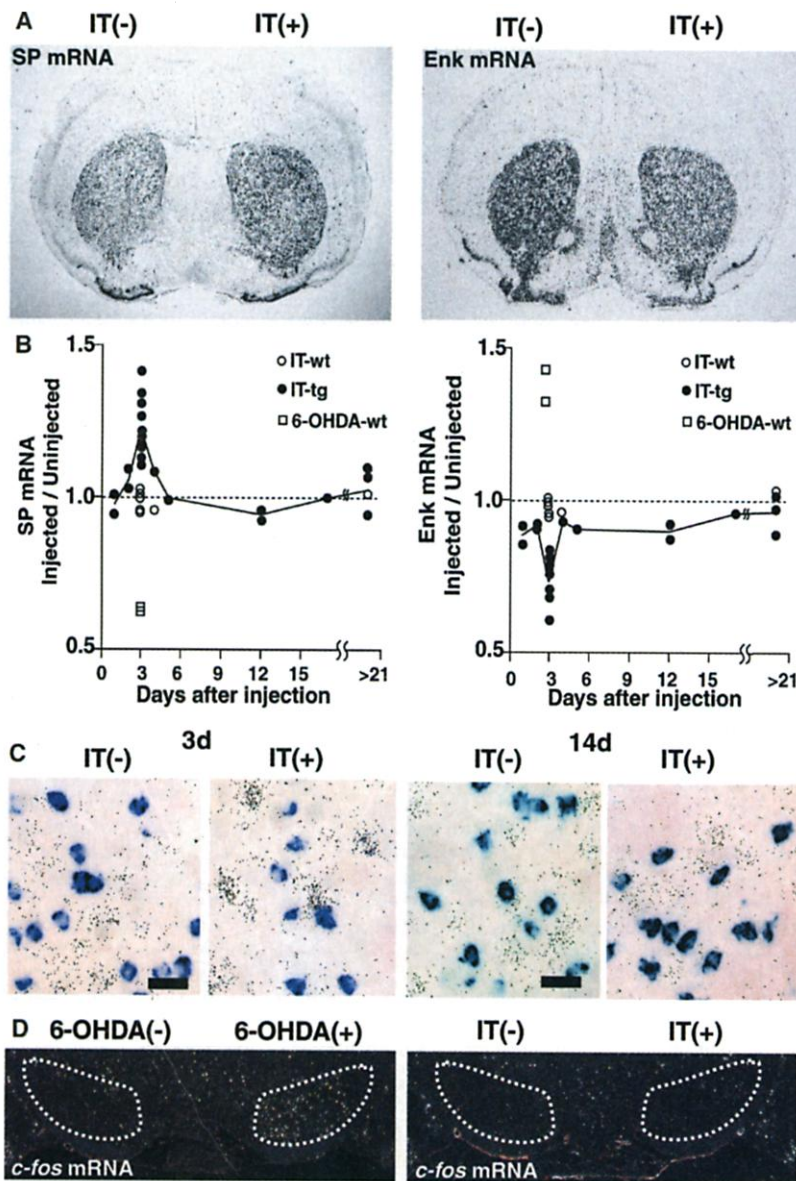


Fig. 3. Differential regulation of SP and Enk mRNAs in the striatum of IT-injected transgenic mice. (A) Bright-field micrographs of in situ hybridization illustrating up-regulation of SP mRNA and down-regulation of Enk mRNA at the IT-injected side in transgenic mice 3 days after IT treatment. (B) IT or 6-OHDA was injected into the left striatum of individual mice at day 0. Each point represents an average of fold changes of mRNA levels determined from five to six brain sections of one animal. SP and Enk mRNA levels were significantly changed at day 3 in both IT- and 6-OHDA-treated mice as compared with IT-treated wild-type mice ($P < 0.01$). (C) Double in situ hybridization on the same striatal section 3 and 14 days after IT treatment with [35 S]-labeled SP mRNA probe (grain) and digoxigenin-labeled Enk mRNA probe (blue). Scale bar, 20 μ m. (D) Up-regulation of *c-fos* mRNA at the SNr/EPN (enclosed) 3 days after intra-striatal injection of 6-OHDA, but no alteration 3 days after IT injection of transgenic mice.

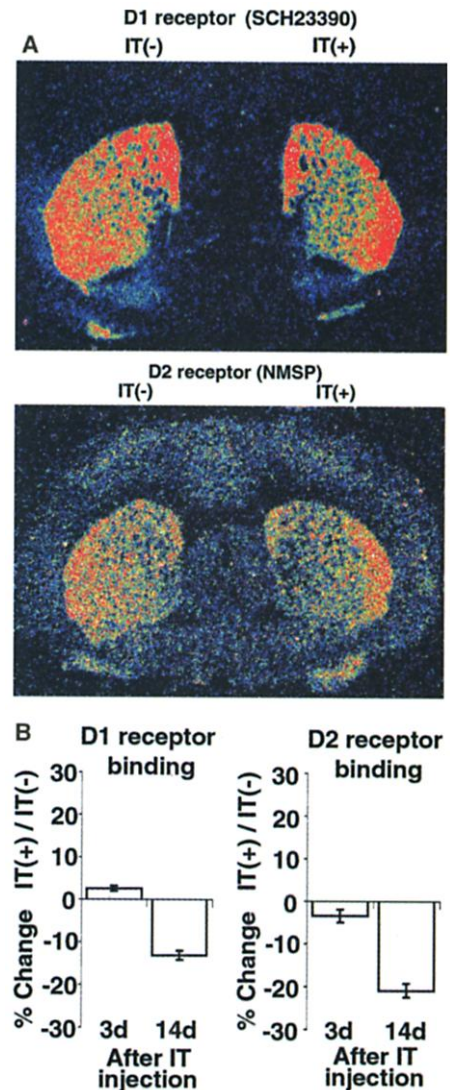


Fig. 4. Adaptive reduction in striatal D1 and D2 receptor levels at the chronic phase of IT treatment. (A) Pseudocolor images of autoradiography showing the binding of [3 H]-labeled D1 and D2 receptor ligands in the striatum at day 14 after IT injection into the left striatum of transgenic mice. (B) Binding levels of D1 and D2 receptors were significantly reduced on day 14 ($P < 0.01$) but not changed on day 3 ($P > 0.90$) at the IT-injected side as compared with the uninjected side of the striatum of transgenic mice. Columns and error bars represent mean \pm SEM, respectively.

respectively (12, 14). Quantitative in situ hybridization analysis of SP and Enk mRNAs was performed (31). At the acute phase, SP and Enk mRNAs increased and decreased at the IT-injected side, respectively (Fig. 3A). Changes in SP and Enk mRNA levels peaked at day 3 after IT treatment and then rapidly returned to normal levels (Fig. 3B), consistent with the time course of an abnormal turning in IT-injected animals. In control experiments, no alteration of SP and Enk mRNA levels was seen in the striatum of IT-injected wild-type mice (Fig. 3B) or of the IT-uninjected side of transgenic mice (27). Furthermore, the expression patterns of both SP and Enk mRNAs were reversed at the acute phase of 6-OHDA-treated striatum (12) (Fig. 3B).

Simultaneous in situ hybridization with differently labeled SP and Enk mRNA probes on the same sections revealed that the neuronal populations expressing the two mRNAs are segregated in both acute phase and chronic phase after IT treatment (Fig. 3C). Hybridization signals of SP and Enk mRNAs increased and decreased, respectively, at the IT-injected side on day 3 and returned to comparable levels between IT-injected and uninjected sides on day 14. mRNA levels of glutamate receptor subunits, NR1, NR2A, GluR1, and GluR2, were also quantitated by in situ hybridization analysis. None of these mRNA levels were altered in the striatum of IT-injected transgenic mice (27). The SNr/EPN neurons receive convergent inputs from the striatonigral and striatopallidal neurons. Reflecting disinhibition of the SNr/EPN neuronal activity after 6-OHDA lesion, *c-fos* mRNA was markedly induced in the SNr/EPN neurons of 6-OHDA-treated animals (Fig. 3D). In contrast, no such induction was

observed at the acute phase of cholinergic cell ablation (Fig. 3D).

In the striatum, the majority of D1 and D2 receptors are localized at the postsynaptic sites of striatal principal neurons (32). To address whether responsiveness to DA is adaptively changed during cholinergic cell elimination, we examined alterations of D1 and D2 receptor binding levels by in vitro quantitative autoradiography (33). In the acute phase of IT treatment, the binding patterns of both D1 receptor–preferring antagonist [³H]-SCH23390 and D2 receptor–preferring antagonist [³H]-*N*-methylspiperone (NMSP) remained unchanged between IT-treated and untreated sides of the striatum (Fig. 4B). In the chronic phase, the binding of both ligands was significantly reduced at the IT-treated side as compared with the untreated side (Fig. 4). No such change was observed in either the acute phase (day 3) or chronic phase (day 14) of IT-treated wild-type mice (27).

Convergence of ACh and DA transmission within the striatum is central to not only basal ganglia function but also to the clinical management of extrapyramidal motor disorders (34). However, previous pharmacological studies produced inconclusive results concerning both turning behavior and regulatory expression of SP and Enk mRNAs in the striatal principal neurons (30, 35, 36). The present investigation with IMCT technology demonstrates that striatal cholinergic neurons are indispensable in controlling striatal neuronal activity and extrapyramidal motor movement. An important finding of this investigation is that an ACh-DA interaction plays a crucial role in both synaptic perturbation and adaptation in the basal ganglia circuit (Fig. 5). D1 and D2 receptors are

segregatedly localized at the postsynaptic sites of striatonigral and striatopallidal neurons, respectively [(12, 37), but see also (38, 39)]. DA therefore excites striatonigral neurons through stimulatory D1 receptors and suppresses striatopallidal neurons through inhibitory D2 receptors (12, 15). In the acute phase, reduction of ACh levels resulted in overwhelming actions of DA within the basal ganglia circuit (Fig. 5A). This DA predominance tended to excite and suppress the striatonigral and striatopallidal neurons, respectively. The resulting imbalance between IT-injected and uninjected sides induced abnormal contralateral rotation. In the chronic phase, adaptation occurred at least partly through the reduction of both D1 and D2 receptors (Fig. 5B). This adaptation relieved imbalance and abolished spontaneous contralateral rotation. However, excess dopaminergic stimulation still produced uncontrolled DA actions at the IT-injected side (Fig. 5C), whereas such stimulation was controlled by antagonistic ACh actions at the intact striatum. Furthermore, dopaminergic inhibition by haloperidol was manifested more at the intact striatum (Fig. 5D), because D1 and D2 receptors were down-regulated at the IT-injected side (Fig. 5B). Therefore, in both cases, the inhibitory output from the SNr/EPN onto the thalamocortical circuit tends to predominate at the IT-uninjected side over the IT-injected side and induces contralateral rotation. Hence, the adaptive synaptic transmission leaves defective responsiveness to both excess stimulation and inhibition of DA actions. Furthermore, our observation regarding distinct responses of SP and Enk mRNAs between acute and chronic phases can explain the seemingly contradictory conclusions of pharmacological experiments (35, 36). We

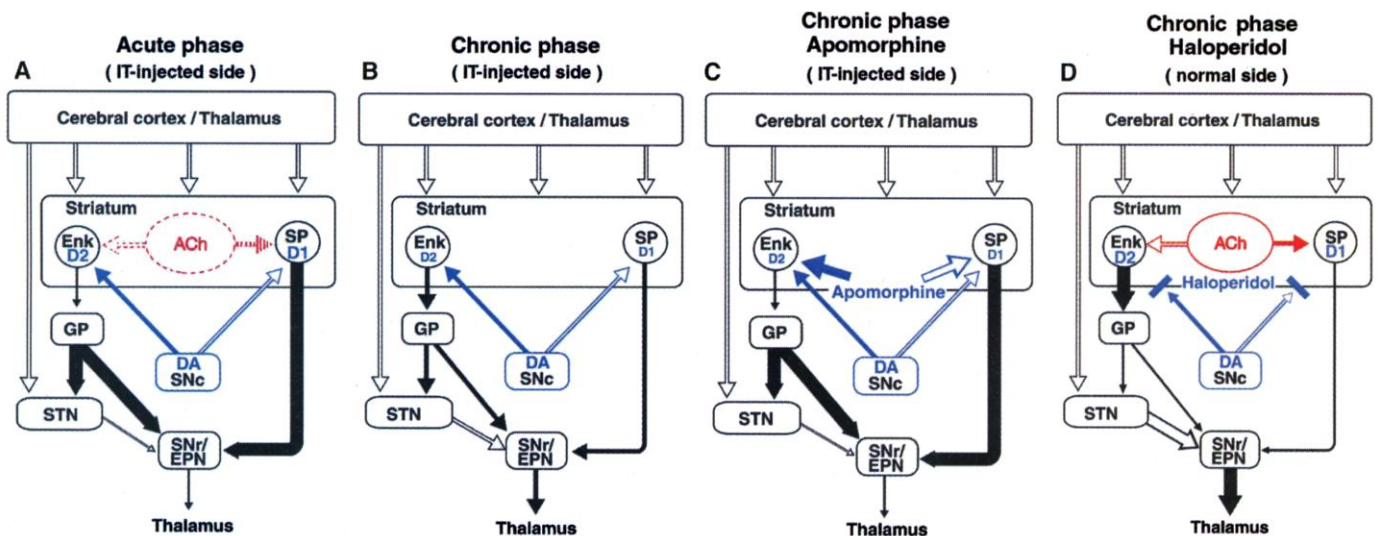


Fig. 5. (A through D) A model for imbalanced and adaptive basal ganglia circuitry after striatal cholinergic cell elimination. Filled and open arrow-headed lines denote the inhibitory and excitatory transmission pathways, respectively. White, glutamate; black, GABA; blue, DA; red, ACh. The

thickness of the lines indicates relative activity of the individual transmission pathway. D1 and D2 indicate DA receptor subtypes. Refer to text for detailed explanation of the indicated model. STN, subthalamic nucleus; GP, globus pallidus; SNc, substantia nigra pars compacta.

REPORTS

previously reported that Golgi cell elimination abolishes GABA-mediated inhibition onto granule cells in the cerebellum (22). This synaptic perturbation is partly compensated by an adaptive attenuation of excitatory N-methyl-D-aspartate receptors in granule cells. These results and the present experiments indicate that synaptic integration in a local circuit is crucially regulated by convergent interactions of distinct neurotransmitters.

DA agonists and ACh antagonists have both been used in treatment of Parkinson's disease (34). Unfortunately, both types of drugs become ineffective at late phases of the disease. The present study demonstrates that a persistent restraint in ACh actions impairs a modulatory effect of DA transmission in the basal ganglia circuit through a convergent ACh-DA interaction. Careful management of ACh antagonists is thus necessary for the treatment of Parkinson's disease.

References and Notes

1. A. M. Graybiel, T. Aosaki, A. W. Flaherty, M. Kimura, *Science* **265**, 1826 (1994).
2. A. M. Graybiel, *Curr. Opin. Neurobiol.* **5**, 733 (1995).
3. J. C. Houk and S. P. Wise, *Cereb. Cortex* **5**, 95 (1995).
4. W. Schultz, P. Apicella, R. Romo, E. Scarnati, in *Models of Information Processing in the Basal Ganglia*, J. C. Houk, J. L. Davis, D. G. Beiser, Eds. (MIT Press, Cambridge, MA, 1995), chap. 2.
5. T. W. Robbins and B. J. Everitt, *Curr. Opin. Neurobiol.* **6**, 228 (1996).
6. R. L. Albin, A. B. Young, J. B. Penney, *Trends Neurosci.* **12**, 366 (1989).
7. M. Hallett, *Can. J. Neurol. Sci.* **20**, 177 (1993).
8. M. F. Chesselet and J. M. Delfs, *Trends Neurosci.* **19**, 417 (1996).
9. T. Wichmann and M. R. DeLong, *Curr. Opin. Neurobiol.* **6**, 751 (1996).
10. G. E. Alexander and M. D. Crutcher, *Trends Neurosci.* **13**, 266 (1990).
11. C. J. Wilson, in *The Synaptic Organization of the Brain*, G. M. Shepherd, Ed. (Oxford Univ. Press, New York, 1998), chap. 9.
12. C. R. Gerfen *et al.*, *Science* **250**, 1429 (1990).
13. G. Di Chiara, M. Morelli, S. Consolo, *Trends Neurosci.* **17**, 228 (1994).
14. H. Steiner and C. R. Gerfen, *Exp. Brain Res.* **123**, 60 (1998).
15. G. S. Robertson, S. R. Vincent, H. C. Fibiger, *Neuroscience* **49**, 285 (1992).
16. V. Bernard, B. Dumartin, E. Lamy, B. Bloch, *Eur. J. Neurosci.* **5**, 1218 (1993).
17. K. Berger, S. Przedborski, J. L. Cadet, *Brain Res. Bull.* **26**, 301 (1991).
18. M. Xu *et al.*, *Cell* **79**, 945 (1994).
19. J. H. Baik *et al.*, *Nature* **377**, 424 (1995).
20. B. Giros, M. Jaber, S. R. Jones, R. M. Wightman, M. G. Caron, *Nature* **379**, 606 (1996).
21. P. E. Phelps, C. R. Houser, J. E. Vaughn, *J. Comp. Neurol.* **238**, 286 (1985).
22. D. Watanabe *et al.*, *Cell* **95**, 17 (1998).
23. H. Ohishi, R. Shigemoto, S. Nakanishi, N. Mizuno, *Neuroscience* **53**, 1009 (1993).
24. Supplemental Web material is available at www.sciencemag.org/feature/data/1051149.shl.
25. K. Kobayashi *et al.*, *Proc. Natl. Acad. Sci. U.S.A.* **92**, 1132 (1995).
26. The IG16 and IG17 lines of heterozygous transgenic mice and their wild-type littermates (22) were deeply anesthetized with sodium pentobarbital at the ages of 7 to 13 weeks. A glass needle was introduced into the left hemisphere with stereotaxic techniques (24), and the anti-Tac(Fv)-PE38 immunotoxin (10 ng/0.5 μ l of PBS) or PBS alone was slowly injected into five points in the left striatum over 3 min. For 6-OHDA treatment, PBS (0.5 μ l) containing 6-OHDA hydrobromide (4 mg/ml) and 0.016% ascorbic acid was injected into two points in the left striatum over 1 min. All procedures were performed according to guidelines of Kyoto University Faculty of Medicine.
27. S. Kaneko, unpublished data.
28. ACh contents in the striatum were measured with radioimmunoassay as described by K. Kawashima, H. Ishikawa, and M. Mochizuki [*J. Pharmacol. Methods* **3**, 115 (1980)]. DA, DOPAC, and HVA contents in the striatum were measured with high-performance liquid chromatography as described by M. Warnhoff [*J. Chromatogr.* **307**, 271 (1984)]. Levels of ACh, DA, DOPAC, and HVA in the intact striatum of wild-type mice were 760 ± 50 , 616 ± 24 , 29.0 ± 0.9 , and 31.7 ± 1.3 pmol/mg of protein (mean \pm SEM), respectively. Statistical analysis was performed by analysis of variance, and post hoc comparisons for this analysis and for histological and behavioral analysis were made with Fisher's protected least significant difference and Scheffé test, respectively.
29. Mice were placed in a round-bottom glass bowl (25 cm in diameter), and rotations were counted for a 5-min period by visual observation. One rotation was defined by the animal completing a 360° circle without turning back to the opposite direction. Apomorphine-HCl (1 mg/kg) and haloperidol (6 mg/kg) were injected 15 min before measuring rotations.
30. C. J. Pycock, *Neuroscience* **5**, 461 (1980).
31. Coronal sections of 10 μ m thickness were prepared by cutting a fresh-frozen brain and mounted onto glass slides. In situ hybridization analysis was performed as described previously (22). Radioactivity of brain sections was quantitated with a microcomputer-coupled image-processing system (BAS5000, Fuji-film). For each section, a rectangular region of interest was set on the corresponding part of both IT-injected and uninjected dorsal striata. Radioactivity measurements were made on serial coronal sections every 100 μ m. Five to six sections were used for each animal to calculate the mean radioactivity of the striatum. Anatomical analysis of [³⁵S]-riboprobe and digoxigenin-labeling hybridization was performed according to procedures described previously (23) and those described by Le Moine and Bloch (37), respectively.
32. A. I. Levey *et al.*, *Proc. Natl. Acad. Sci. U.S.A.* **90**, 8861 (1993).
33. Quantitative autoradiography of D1 and D2 receptor [³H]-ligand binding was performed as described by Berger *et al.* (17) with a minor modification. Quantification of autoradiographs was done essentially as described for in situ hybridization analysis.
34. S. Fahn, R. Burke, Y. Stern, *Prog. Brain Res.* **84**, 389 (1990).
35. L. K. Nisenbaum, S. T. Kitai, C. R. Gerfen, *Neuroscience* **63**, 435 (1994).
36. J. Q. Wang and J. F. McGinty, *Brain Res.* **748**, 62 (1997).
37. C. Le Moine and B. Bloch, *J. Comp. Neurol.* **355**, 418 (1995).
38. D. J. Surmeier, A. Reiner, M. S. Levine, M. A. Ariano, *Trends Neurosci.* **16**, 299 (1993).
39. O. Aizman *et al.*, *Nature Neurosci.* **3**, 226 (2000).
40. We thank K. K. Dev and K. Kobayashi for valuable advice and K. Kawashima for a gift of ACh antibody and [³H]-ACh. This work was supported in part by research grants from the Ministry of Education, Science and Culture of Japan and the International Resource Program of the National Cancer Institute.

10 April 2000; accepted 31 May 2000

So instant, you don't need water...

NEW! Science Online's Content Alert Service: The only source for instant updates on breaking science news. This free *Science* Online enhancement e-mails summaries of the latest research articles published weekly in *Science* – **instantly**. To sign up for the Content Alert service, go to *Science* Online – and save the water for your coffee.

Science
www.sciencemag.org

For more information about Content Alerts go to www.sciencemag.org. Click on Subscription button, then click on Content Alert button.